


## Article

# Sealing Performance Analysis of an End Fitting for Marine Unbonded Flexible Pipes Based on Hydraulic-Thermal Finite Element Modeling

Liping Tang <sup>1</sup>, Wei He <sup>1</sup>, Xiaohua Zhu <sup>1,\*</sup> and Yunlai Zhou <sup>2</sup> 

<sup>1</sup> School of Mechatronic Engineering, Southwest Petroleum University, Chengdu 610500, China; lipingtang@swpu.edu.cn (L.T.); hewei@stu.swpu.edu.cn (W.H.)

<sup>2</sup> Department of Civil and Environmental Engineering, The Hong Kong Polytechnic University, Hong Kong 00852, SAR, China; YunLai.zhou@alumnos.upm.es

\* Correspondence: zhuxh@swpu.edu.cn

Received: 11 May 2019; Accepted: 30 May 2019; Published: 10 June 2019



**Abstract:** End fittings are essential components in marine flexible pipe systems, performing the two main functions of connecting and sealing. To investigate the sealing principle and the influence of the temperature on the sealing performance, a hydraulic-thermal finite element (FE) model for the end fitting sealing structure was developed. The sealing mechanism of the end fitting was revealed by simulating the sealing behavior under the pressure penetration criteria. To investigate the effect of temperature, the sealing behavior of the sealing ring under different temperature fields was analyzed and discussed. The results showed that the contact pressure of path 1 (i.e., metal-to-polymer seal) was 31.7 MPa, which was much lower than that of path 2 (metal-to-metal seal) at 195.6 MPa. It was indicated that the sealing capacities were different for the two leak paths, and that the sealing performance of the metal-to-polymer interface had more complicated characteristics. Results also showed that the finite element analysis can be used in conjunction with pressure penetration criteria to evaluate the sealing capacity. According to the model, when the fluid pressures are 20 and 30 MPa, no leakage occurs in the sealing structure, while the sealing structure fails at the fluid pressure of 40 MPa. In addition, it was shown that temperature plays a significant role in the thermal deformation of a sealing structure under a temperature field and that an appropriately high temperature can increase the sealing capacity.

**Keywords:** end fitting; unbonded flexible pipe; sealing performance; pressure penetration; temperature

## 1. Introduction

The development of offshore resources has traditionally relied on floating production systems, such as floating production storage and offloading (FPSO) units and semi-submerged ships [1]. The hydrocarbons produced by an FPSO or from nearby subsea templates are transported through a pipeline or offloaded onto a tanker [2,3]. In terms of offshore pipes, submarine pipelines, which are buried in a trench or laid on the seabed, are commonly used [4,5]. Compared with conventional steel pipes, flexible pipe systems have the characteristics of higher flexibility, greater applicability, and enhanced recyclability [6]. Flexible pipes can be classified into two primary types: bonded flexible pipes and unbonded flexible pipes [7,8]. An unbonded flexible pipe usually comprises an outer polymeric layer, helical tensile armor, anti-wear layers, pressure armor layers, and an inner carcass layer [9], as shown in Figure 1. With the rapid development of techniques for exploiting deep-water resources, unbonded flexible pipes now play a significant role in transferring oil and gas resources from offshore platforms to onshore facilities.

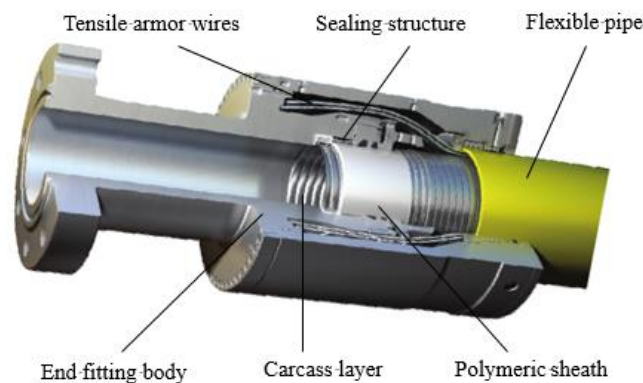


**Figure 1.** Typical cross-section of flexible pipeline end fitting [9].

Connecting the subsea infrastructure to surface facilities and transporting hydrocarbon products are the major applications of flexible pipes in the offshore oil and gas industry [10]. However, the harsh deep-sea environment imposes significant challenges on flexible pipes, necessitating higher mechanical response and performance characteristics [11]. According to the American Petroleum Institute (API), the terminations of a flexible pipe are defined as end fittings (as shown in Figure 2), of which the functions are: (1) to provide a transition between the pipe body and the connecting component and (2) to transmit the loads acting on the pipe without allowing the pipe to fail [12]. The widespread use of flexible pipes under more demanding operational conditions makes the safety performance of end fittings particularly important [13].

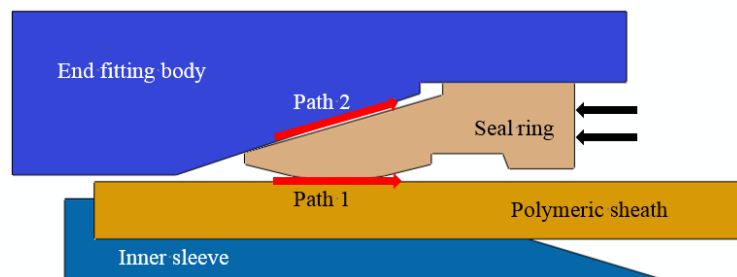


**Figure 2.** Schematic illustration of the sealing structure.

Experiences in offshore environments have shown that the end fitting of a flexible pipe may be the weakest point [13]. In service, end fittings will be subjected to similar environmental loads and conditions as the pipe, such as axial tension, inner pressure, and external hydrostatic pressure [14]. Apart from mechanical load, the end fitting has to offer thermal insulation and be leak-proof [13]. Therefore, if the sealing capacity of the end fitting is insufficient, there will be a risk of oil and gas leakage, which can have serious consequences. Because the composite structure of flexible pipe consists of many independent concentric metallic and polymeric layers, the structure of the end fitting is also multifaceted and complex [15]. To ensure that the end fitting has adequate sealing performance, it is necessary to investigate its sealing capacity.

In general, existing studies related to the sealing performance of a structure have concentrated on the sealing rings [16]. Typical examples are “O” rings, although these are different from the structure of an end fitting sealing assembly. In addition, a number of studies have focused on the mechanical behavior of flexible pipe, such as the instability of the armor wire [17], the collapse of the carcass layers [18], and fatigue reliability analysis [19]. Although the sealing behavior of the end fitting is unlike the mechanical behavior of the flexible pipe body or the layers inside the end fitting, which have been extensively investigated [8,20], there has been relatively little research on the sealing performance of the end fittings themselves.

The composite materials used in flexible pipe have different properties to metallic materials in terms of anisotropy, thermal expansion coefficient, thermal conductivity, and stiffness. Indeed, the structural properties of composite materials are more complex than those of metallic materials. This may lead to interface failure, such as when the composite material separates from the metallic material, thus losing the ability to maintain leak-tight integrity. Hatton et al. [15] studied the design of sealing assemblies in different types of end fittings using finite element (FE) analysis and laboratory testing.

To understand the sealing performance of a mechanical connector in a subsea pipeline, Wang et al. [21] investigated the critical condition of the sealing structure and created a new method to analyze the contact pressure of the sealing surface by examining the static metal sealing mechanism. An optimized design for a new subsea pipeline mechanical connector was proposed and an approach for determining the contact pressure of various dimensions was provided.

For an end fitting in a high-pressure pipe, it is challenging to create the necessary sealing performance. Fernando et al. [22] developed an FE model of a flexible pipe end fitting and presented a method of evaluating the sealing performance of the sealing assembly and the design requirements for the sealing assembly of the end fitting. In their work, FE analysis was conducted using specially established leak criteria. In addition, an ultrasonic technique was used to measure the contact pressure at the metal-to-metal interface, which showed that their method had significant promise.

Li et al. [23] considered the sealing performance of the sealing assembly in a deep-water flexible pipe end fitting and established an FE model using the ABAQUS software (6.11). They studied the key parameters under different conditions, providing further references for research on flexible pipe end fittings. By summarizing the general sealing criteria, Zhang [24] introduced the concept of “contact pressure amplification factor” to evaluate the sealing capability of end fittings, while Marion et al. [25] investigated the suitability of end fittings for high-temperature thermal cycling conditions using specially designed pipe samples and facilities that satisfy the API specifications.

Previous studies have analyzed and optimized the sealing criteria and the geometric parameters of the sealing assembly. However, there have been few studies related to the sealing behavior. In general, research on the sealing performance of the end fittings is not comprehensive. In this study, FE methods were used to develop a two-dimensional axisymmetric numerical model of the sealing structure of an end fitting, including the temperature field. The pressure penetration criteria were applied to this model to analyze the performance of the sealing structure.

## 2. Sealing Analysis

### 2.1. Sealing Structure

According to the API SPEC 17J and 17B standards [12,26], the sealing structure of a typical flanged unbonded flexible pipe end fitting is as illustrated in Figure 2. As can be seen in the figure, the functional structure of the sealing system is mainly composed of four parts: the inner sleeve, polymeric sheath, sealing ring, and end fitting body. The inner sleeve is the innermost component of the end fitting. This plays a supporting role in the whole structure and is used to bear the radial force while in service. The polymeric sheath of the flexible pipe is pressed on the outer side of the inner sleeve, and is one of the most important parts of the sealing structure. The end fitting body is the outermost part of the sealing structure, and is used to protect all components in the end fitting. The wedge sealing ring provides the critical sealing capacity through axial extrusion.

The sealing ring is designed in advance according to the specifications of the flexible pipe and end fitting. The sealing assembly in an end fitting is usually formed by swaging a metallic sealing ring into the area between the polymeric layer and the end fitting body. During assembly, the contact surface between the sealing ring and the end fitting body and between the sealing ring and the polymeric sheath creates two leakage paths [14,22]. Path 2 is the metal-to-metal microscopic gap between the end fitting body and the sealing ring, where a higher contact pressure ensures better sealing capacity. Path 1 refers to the metal-to-polymer contact interface between the sealing ring and the polymeric

sheath of the flexible pipe. This path involves complex interactions such as elastic–plastic deformation and nonlinear contact. The contact pressure is lower than in path 1, so leaks are more likely to occur through this path.

## 2.2. Sealing Criteria

Sealing can be either dynamic or static. The contact sealing between the sealing ring and the polymeric material in the inner layer of the flexible pipe is a type of static sealing [27]. In engineering applications, the performance of this type of sealing is evaluated by comparing the contact pressure and the length of the two contact surfaces. To obtain good sealing capacity, it is necessary to achieve a relatively large contact pressure, and so the length of the contact surface should be as long as possible. Of course, the premise is that the physical properties of the material itself cannot be destroyed.

For the sealing to remain valid, the contact pressure of the sealing path must be greater than the critical failure pressure. However, calculating the critical failure pressure is complicated, and the influence of the material and the medium should be considered. In a previous study [22], the nominal critical failure pressure was expressed as

$$p_c = \alpha p_f + (1 - \alpha) \sigma_Y \quad (1)$$

where  $p_c$  is the critical failure pressure and  $p_f$  is the fluid pressure in the sealing system,  $\sigma_Y$  is the smaller yield stress of the two materials in contact, and  $\alpha$  is the ratio of the length of the fluid infiltrating into the contact surface to the length of the contact path. However, in practical applications, the geometry and roughness of the contact surface exert significant influences, so this formula is not exact.

In this study, to simulate the real process of fluid intrusion, a pressure penetration module was employed in the FE software [28,29]. The loading principle of the pressure penetration criteria is illustrated in Figure 3. On the two contact surfaces, the surface with elements 3 and 4 is defined as the master surface, and that with elements 1 and 2 is defined as the slave surface. Nodes 11 and 12 belong to element 1 on the side of the contact surface.

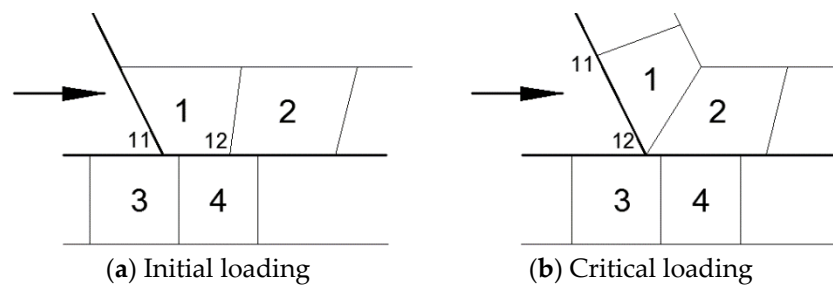


Figure 3. Pressure penetration criteria diagram.

As shown by the arrows in this figure, when the fluid penetrates from left to right, the fluid pressure load will be applied normal to the surface from left to right. Node 11 is the first node exposed to the fluid pressure. If the contact pressure of node 11 is higher than the applied fluid pressure, the pressure penetration stops and node 11 becomes the critical node for the contact pressure (Figure 3a). If the contact pressure of node 11 is less than the fluid pressure, the pressure penetration will continue to load along the contact surface until a new critical contact pressure node is reached (Figure 3b). In addition, if no critical node exists, the contact path cannot provide the sealing capacity under this fluid pressure. The application of pressure penetration can identify the critical node dynamically along the path and determine whether the sealing capacity is sufficient [30].

## 2.3. Thermal Sealing Analysis

High temperatures will lead to thermal expansion and material deformation, which will change the contact behavior and affect the sealing performance [31]. However, in previous studies on the

sealing performance of end fittings, temperature has seldom been taken into account. Over recent years, operating temperatures and pressures have risen as water depths have continued to increase, making the design, manufacture, and installation of flexible pipe a complex challenge. Therefore, the thermal sealing performance at different temperatures is investigated in this paper. Changes in temperature should follow the basic thermal conduction equation. According to the law of conservation of energy, this can be calculated as follows [32]:

$$\rho c \frac{\partial \theta}{\partial t} = \frac{\partial}{\partial x} \left( k \frac{\partial \theta}{\partial x} \right) + q(x, t) \quad (2)$$

At the same time, the FE method has the ability to model heat transfer with convection. Based on the work of Yu and Heinrich [33,34], the formulation can be obtained by the following expression:

$$\int \delta \theta \left[ \rho c \left\{ \frac{\partial \theta}{\partial t} + V \cdot \frac{\partial \theta}{\partial x} \right\} - \frac{\partial}{\partial x} \cdot \left( k \cdot \frac{\partial \theta}{\partial x} \right) - q \right] dV + \int_{S_q} \delta \theta \left[ n \cdot k \cdot \frac{\partial \theta}{\partial x} - q_s \right] dS = 0 \quad (3)$$

where  $c(\theta)$  is the specific heat capacity of the fluid,  $\rho(\theta)$  is the fluid density,  $\theta(x, t)$  is the temperature at a spatial position  $x$  at time  $t$ ,  $k(\theta)$  is the conductivity of the fluid,  $q(x, t)$  is the heat added per unit volume from external sources,  $\delta \theta(x, t)$  is an arbitrary variational field,  $q_s$  is the heat flowing into the volume across the surface on which the temperature is not prescribed ( $S_q$ ), and  $n$  is the outward normal to the surface.

The boundary condition of this thermal equilibrium equation is that  $\theta(x)$  is prescribed over some part of the surface  $S_\theta$ , and that the heat flux per unit area entering the domain across the rest of the surface,  $q_s(x)$ , is defined by convection or radiation conditions. In the conditions considered in this study, the boundary term in the equation defines

$$q_s = -n \cdot k \cdot \frac{\partial \theta}{\partial x} \quad (4)$$

This implies that  $q_s$  is the flux associated with conduction across the surface only; any convection of energy across the surface is not included in  $q_s$ .

#### 2.4. Mechanical Analysis

Based on the analysis of the flexible pipe end fitting sealing structure in the preceding section, the polymeric sheath is squeezed between the inner sleeve and the end fitting body when assembled. Thus, in the FE model, the axial degrees of freedom at both ends of the polymeric sheath are restrained to prevent axial motions, but radial free expansion and contraction are not affected. When variations in temperature lead to thermal deformation of the polymeric sheath, the expansion can only happen in the radial direction. In previous studies on the deformation of polymeric material [27], the radial deformation of the seal can be calculated by converting the deformation in the axial direction to a deformation in the radial direction. Based on the principle of volume invariance, the deformation relation between the radial direction and the axial direction for a cylinder specimen can be described as

$$\frac{\pi d^2}{4} (l + \Delta l) = \frac{\pi (d + \Delta d)^2}{4} l \quad (5)$$

where  $d$  is the diameter of the cylinder specimen before the deformation,  $l$  is the length of the cylinder specimen before deformation, and  $\Delta d$  and  $\Delta l$  are the radial and axial increments, respectively, of the cylinder specimen after deformation.

### 3. FE Modeling Procedures

Considering the geometry and axisymmetric load characteristics of the sealing system, a two-dimensional plane axisymmetric solid model is employed to predict the seal performance. This section describes a thermal coupling sealing structure model of a flexible pipe with a design pressure of 20 MPa. This model was developed using FE with the ABAQUS software. Note that the factory acceptance test pressure is 1.5 times the design pressure, so the critical pressure acting on the end fitting is 30 MPa in service [12]. The model comprises the inner sleeve, polymeric sheath, sealing ring, and end fitting body, from inside to outside. The inner and outer diameters of the flexible pipe are 139.7 mm and 209.5 mm, respectively, and the thickness of the polymeric sheath is 5 mm. The basic physical properties of each component are listed in Table 1.

**Table 1.** Materials and properties for each part of the model.

Component	Young's Modulus (GPa)	Poisson's Ratio	Yield Strength (MPa)
End fitting body	210	0.3	355
inner sleeve	210	0.3	355
Sealing ring	191	0.3	758
Polymeric sheath	0.571	0.45	20.74

In addition, the polymeric sheath of the flexible pipe is usually made from high-molecular-weight polymeric materials, such as high-density polyethylene (HDPE) [35]. In this study, the polymeric material parameters were taken from the work of Malta and Martins [36], and the elastic–plastic properties are illustrated in Figure 4.

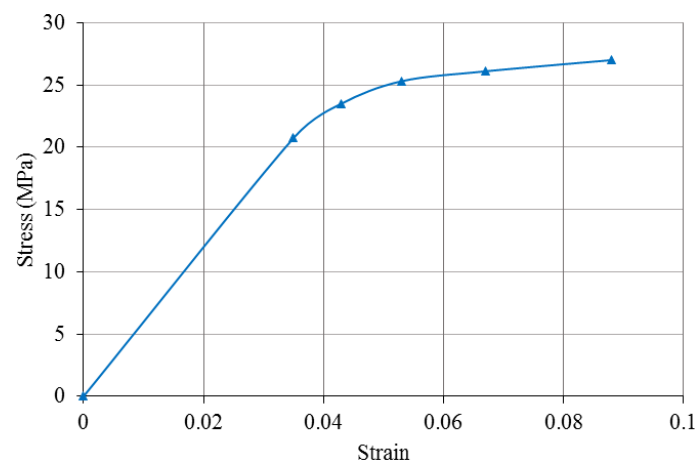


**Figure 4.** Stress versus strain curve for the polymeric material [36].

To model the incompressible or quasi-incompressible characteristics of these materials, the planar axisymmetric hybrid element CAX4H is selected. Structured and sweep meshing techniques are used in each part of the model, and the mesh is refined around the contact area to improve the accuracy of the simulation. Because of the nonlinear contact characteristics of metallic and polymeric materials, the Mohr-Coulomb friction criterion is employed to describe the contact relationship (i.e., normal contact is “hard” and tangential contact incurs a penalty under a friction coefficient of 0.1) [37].

To simulate the sealing process of the sealing ring, full constraints are applied to the inner sleeve, end fitting body, and polymeric sheath of the flexible pipe, while the sealing ring is free to undergo axial displacement. Pressure penetration is then applied to predict the effectiveness of the sealing. When analyzing the parameter sensitivity of the sealing structure, a temperature field is applied to the model. In addition, an implicit solver is used to obtain improved solution convergence and performance. The FE model of the sealing structure is illustrated in Figure 5.



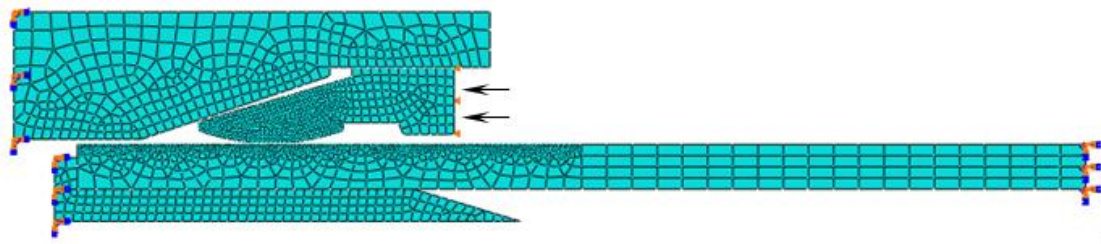


Figure 5. Description of the finite element (FE) model.

## 4. Results and Discussion

### 4.1. Simulation of Sealing Principle

According to the design specifications and assembly requirements of the end fitting, axial displacement is applied to the sealing ring to achieve an interference fit. In this section, the von Mises stress and the contact pressure of the model are investigated to analyze the sealing performance of the sealing structure. The von Mises stress distribution of the sealing structure after assembly at 20 °C is shown in Figure 6.

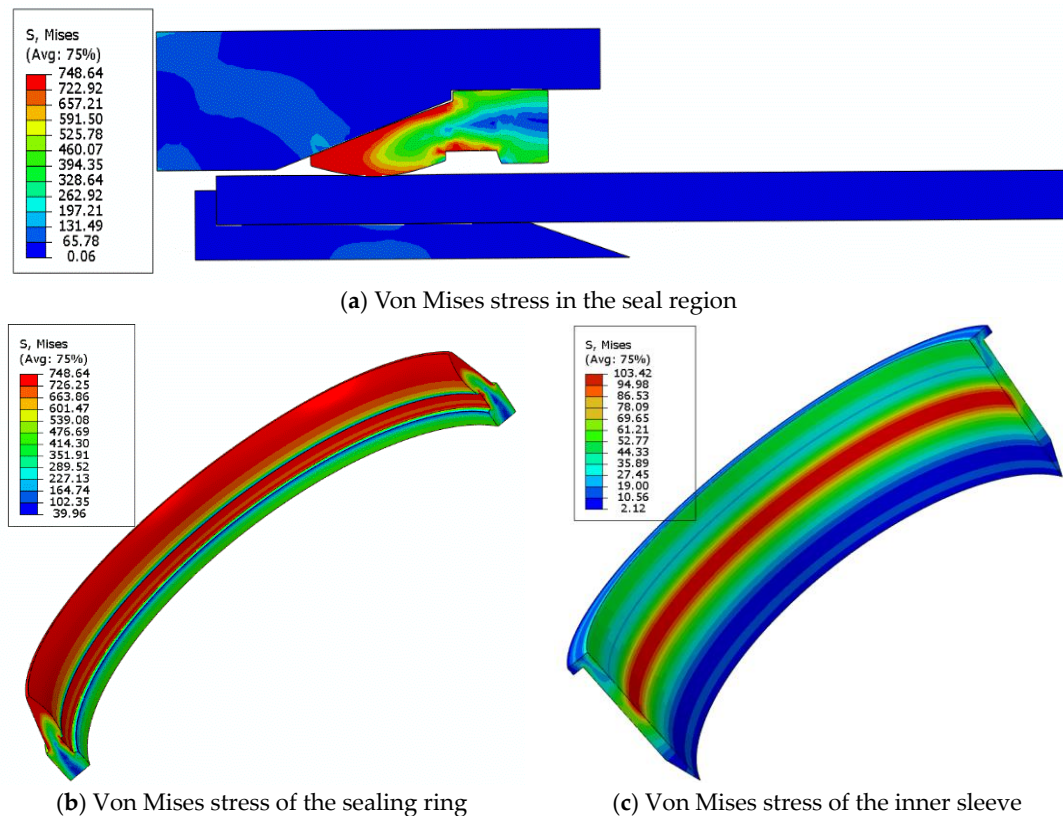


Figure 6. Von Mises stress distribution of the FE model.

As can be seen from Figure 6a, the von Mises stress of the model is mainly concentrated on the wedge sealing ring, and so the stress of the inner sleeve and the end fitting body is relatively small. The closer to the tip of the sealing ring, the greater the von Mises stress, because the tip is subjected to a greater pressure. A three-dimensional von Mises stress contour distribution of the sealing ring, obtained by rotating the planar sealing ring, is shown in Figure 6b. The maximum von Mises stress of the wedge sealing ring is 748.6 MPa in the FE model, which does not exceed the yield stress of the material. This shows that no plastic deformation occurs in the sealing ring and the property of the material itself is not destroyed. In addition, some stress concentration occurs in the contact area of

the inner sleeve (as shown in Figure 6c), but the maximum stress is still less than the yield stress of the material.

To clarify the characteristics of the contact pressure distribution in the sealing structure, the three-dimensional contact pressure contour distribution of the FE model is presented in Figure 7. On the polymeric sheath of the flexible pipe, some contact pressure occurs on the outer side of the contact region, although the contact pressure on the inner side is lower. For the sealing ring, the contact pressure is higher on the outer interface close to the end fitting body (i.e., path 2), whereas the contact pressure is lower on the inner interface close to the polymeric sheath (i.e., path 1). This may be caused by the property of the materials along the contact paths.

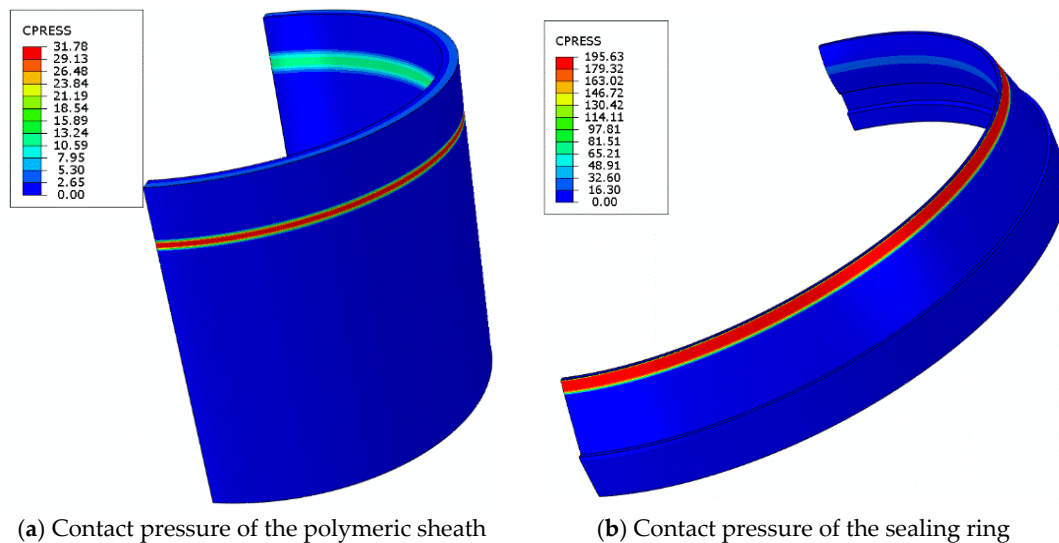


Figure 7. Contact analysis of the sealing structure.

Based on the FE model of the sealing structure, the contact pressure distributions on the nodes along the two paths were obtained. They are illustrated in Figure 8. The maximum contact pressure along path 1 is 31.74 MPa, which is slightly greater than the test pressure of 30 MPa. The maximum contact pressure along path 2 is 195.6 MPa, which is much larger than the design pressure and test pressure of the end fitting. This indicates that there will be no seal leakage along this path, which is consistent with the results of previous works [22,23]. Hence, we focus on path 1 in the following analysis.

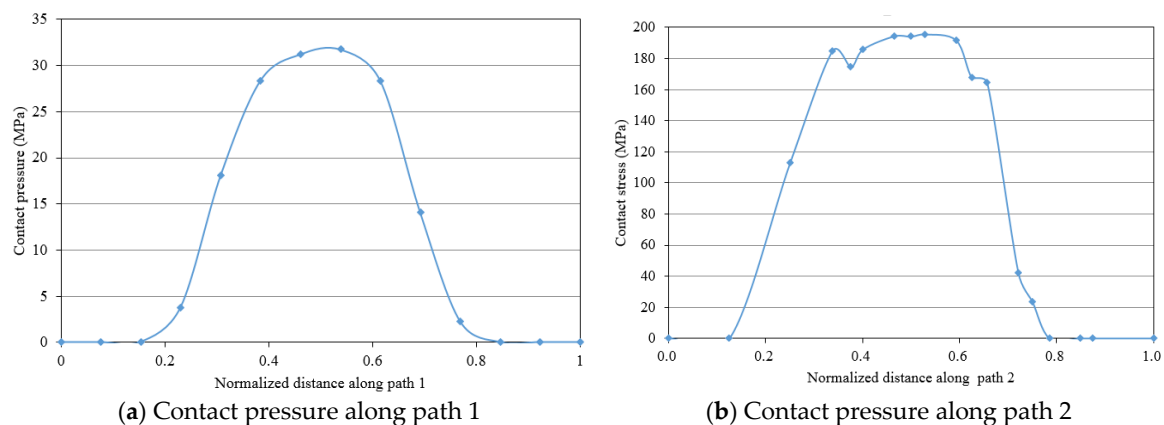
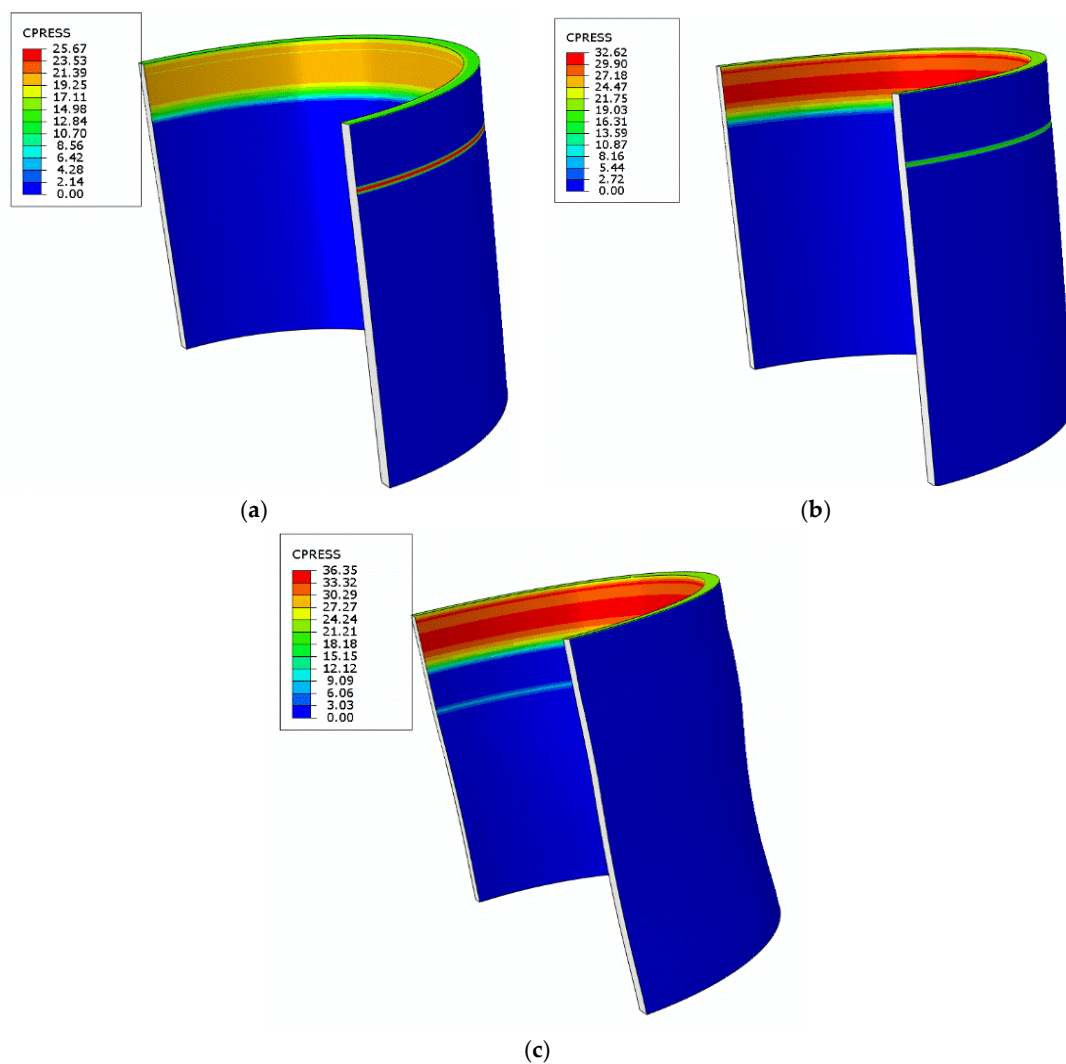


Figure 8. Comparison of the sealing performance along the two paths.



#### 4.2. Analysis of Pressure Penetration

The pressure penetration criteria can be applied to evaluate the sealing capacity of the sealing assembly. According to the design pressure and the maximum test pressure of the end fitting, the sealing performance of the sealing structure along path 1 was analyzed at fluid pressures of 20, 30, and 40 MPa at a temperature of 20 °C. The contact pressure on the polymeric sheath reflects the variation in the pressure penetration, and Figure 9 shows the contact pressure of the polymeric sheath under the different fluid pressures. With an increase in fluid pressure, the contact pressure on one side of the inner surface of the polymeric sheath increases, whereas the pressure on the outer surface gradually decreases. This is because when the fluid acts along path 1, the contact surface between the sealing ring and the polymeric sheath is continuously penetrated by the pressure, causing these components to separate from each other. On the contrary, the contact surface between the sheath and the inner sleeve is squeezed and shrunk along the radial direction.



**Figure 9.** Contact pressure of polymeric sheath under different fluid pressures: (a) 20 MPa; (b) 30 MPa; (c) 40 MPa.

Figure 10 shows the contact pressure distribution of the nodes along path 1. When no pressure penetration is applied, the maximum contact pressure is 31.7 MPa. At fluid pressures of 20 and 30 MPa, the maximum contact pressure and contact length decrease, and the pressure distribution moves to

the right. At this time, the existence of the contact pressure indicates that no leakage will occur in the sealing structure.

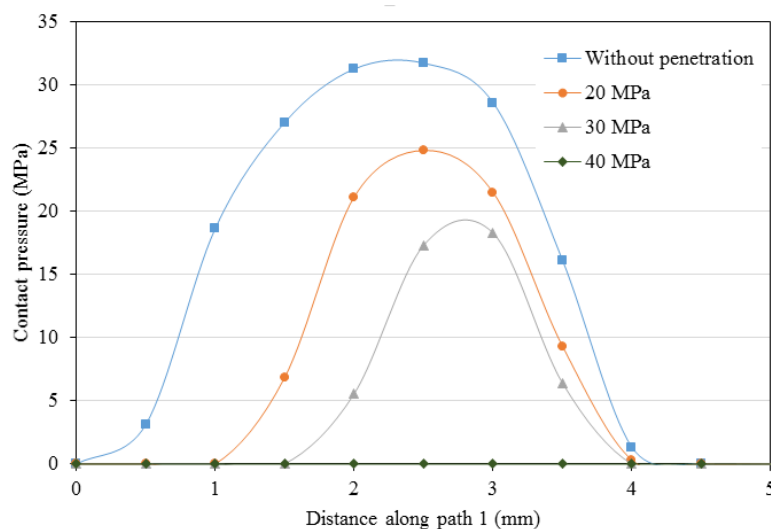


Figure 10. Contact pressure under different fluid pressure.

When the fluid pressure is 40 MPa, the contact pressure along path 1 becomes 0 MPa, which indicates that the fluid pressure is too high, and the sealing structure fails. As shown in Figure 9, the fluid leakage through this path flows around the annulus of the flexible pipe, acting to compress the polymeric sheath and make it collapse. In addition, leakage accidents may occur if the sealing structure fails. It should be emphasized that, after many simulation calculations and predictions, the sealing structure was found to leak at a fluid pressure of 35.5 MPa. In other words, the critical fluid pressure of the sealing structure in this study is 35.5 MPa.

#### 4.3. Analysis of the Thermal Sealing

Under the actual working conditions of flexible pipe end fittings, the hydrocarbon products transported along the pipe can reach high temperatures, so thermal effects in the sealing structure cannot be ignored. This section reports the changes in sealing performance of the sealing structure under temperature fields of 20, 50, 60, 70, and 80 °C in the model [38].

Compared with metallic materials, the polymeric materials in the flexible pipe will be more strongly influenced by temperature. Therefore, after applying different temperature fields to the FE model of the sealing structure, the contact pressure distributions of the polymeric sheath were recorded (as shown in Figure 11). From the perspective of deformation, an increase in temperature deforms the polymeric sheath and causes the flexible pipe to expand. Regarding the contact pressure along path 1, as the temperature increases from 20–80 °C, the maximum contact pressure increases from 31.7–41.3 MPa—a rise of 30% (as shown in Figure 12). In addition, the contact length increases because the material expands at higher temperatures, increasing the number of contactable nodes.

From the results in Table 2, the maximum von Mises stress of the model exhibits a continuous increase, becoming close to the yield strength of the material at 80 °C. The contact pressures along the two paths gradually increase, which indicates that the sealing capacity is also increasing. In summary, thermal effects can enhance the sealing performance, but the temperature should not exceed the rated temperature of the material, otherwise failure will occur.

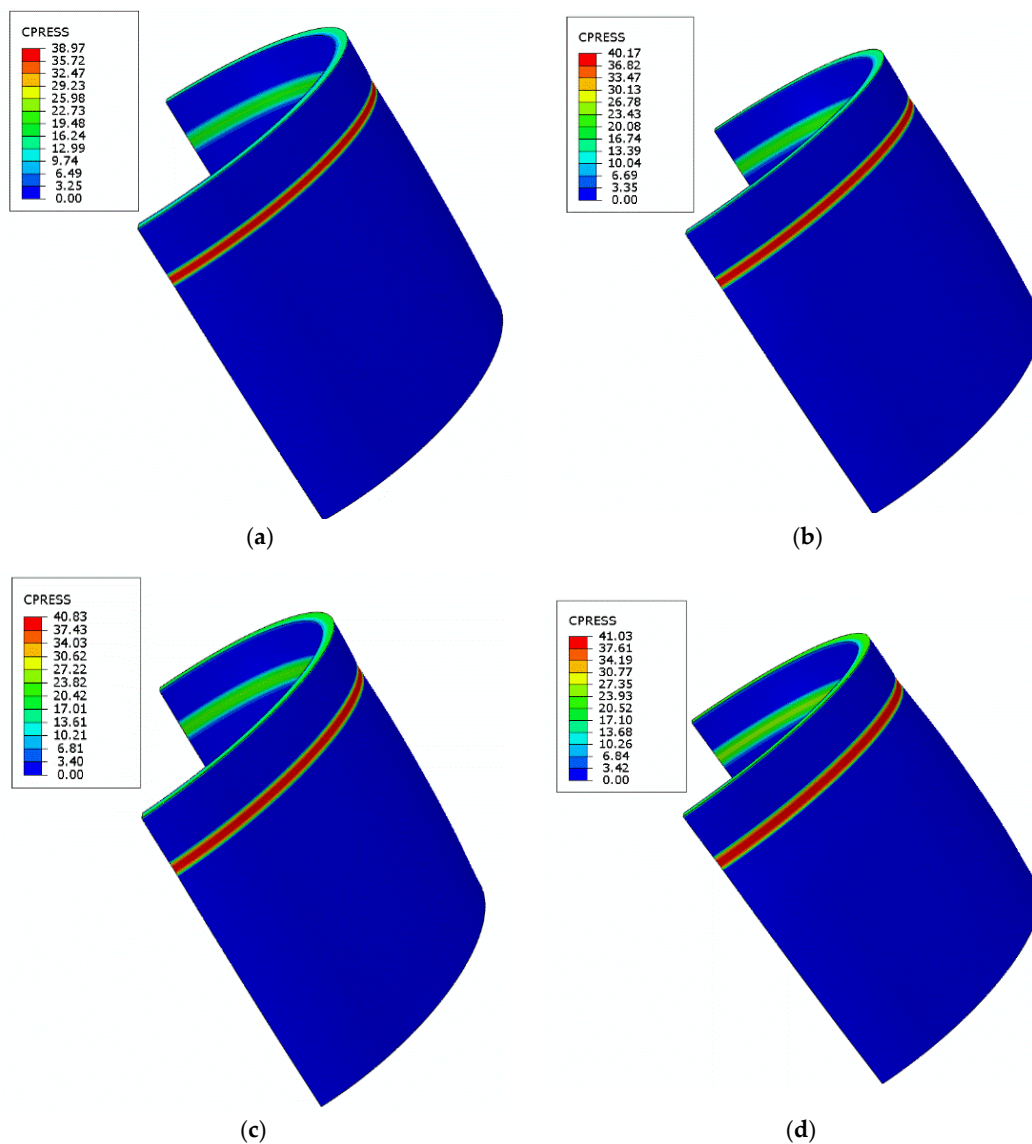


**Figure 11.** Contact pressure distribution of the polymeric sheath: (a) 50 °C; (b) 60 °C; (c) 70 °C; (d) 80 °C.

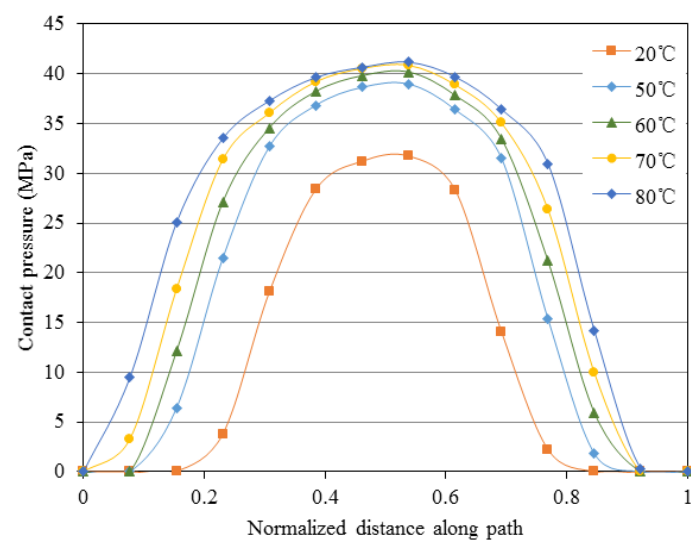


**Figure 12.** Contact pressure along path 1.

**Table 2.** Results of the FE model at different temperatures.

Temperature (°C)	20	50	60	70	80
Von Mises stress (MPa)	748.6	750.1	751.6	753.7	756.8
Contact pressure in path 1 (MPa)	31.7	38.9	40.1	40.8	41.3
Contact pressure in path 2 (MPa)	195.6	199.7	227.3	229.4	234.5

## 5. Conclusions

A classical unbonded flexible pipe is a combination of polymeric and metallic layers. An end fitting with reliable sealing properties is a precondition of a successful flexible pipe application. In this study, a hydraulic-thermal FE model was developed to investigate the sealing performance of a flexible pipe end fitting. The FE model employed the pressure penetration criterion and considered the temperature field, which is suitable for real applications. Using this model, the sealing principle was simulated and the influence of thermal effects on the sealing capacity was investigated.

The results showed that the maximum von Mises stress occurs on the sealing ring during the sealing process, whereas the stresses on the other components are relatively small. In terms of the contact pressure distribution, the maximum value appears in the sealing region, and is higher along path 2. By introducing pressure penetration, the sealing performance could be predicted and the dynamical pressure critical node was identified. In the model described in this paper, the critical fluid pressure of the end fitting is 35.5 MPa, which means that leakage occurs when the working pressure exceeds this value. In previous studies, thermal effects were usually omitted. The results in this paper, however, show that temperature is an important factor in the sealing performance of the sealing assembly, and should not be neglected. Thermal effects cause the components of the sealing structure to deform and expand. By increasing the contact length and contact pressure, the sealing ability of the sealing structure can be improved. Of course, very high temperatures are not appropriate, because the strain on the sealing ring should be considered in actual applications.

**Author Contributions:** L.T. contributed significantly to analysis and manuscript writing; W.H. performed the numerical simulation and data analyses; X.Z. contributed to the conception of the investigation; Y.Z. helped perform the analysis with constructive discussions.

**Funding:** This research was funded by the China Postdoctoral Science Foundation (43XB3793XB), National Key Research and Development Program (2018YFC0310204), National Natural Science Foundation of China (No. 51674214), and Scientific Innovation Group for Youths of Sichuan Province (No. 2019JDTD0017). And The APC was funded by National Key Research and Development Program (2018YFC0310204).

**Conflicts of Interest:** This article does not involve conflicts of interest.

## References

1. Moan, T.; Amdahl, J.; Ersdal, G. Assessment of ship impact risk to offshore structures-New NORSOK N-003 guidelines. *Mar. Struct.* **2019**, *63*, 480–494. [\[CrossRef\]](#)
2. Yang, C.K.; Kim, M.H. Numerical assessment of the global performance of spar and FPSO connected by horizontal pipeline bundle. *Ocean Eng.* **2018**, *159*, 150–164. [\[CrossRef\]](#)
3. Zhang, J.M.; Li, X.S.; Chen, Z.Y.; Zhang, Y.; Li, G.; Yan, K.F.; Lv, T. Gas-Lifting characteristics of methane-water mixture and its potential application for self-eruption production of marine natural gas hydrates. *Energies* **2018**, *11*, 240. [\[CrossRef\]](#)
4. Guha, I.; White, D.J.; Randolph, M.F. Subsea pipeline walking with velocity dependent seabed friction. *Appl. Ocean Res.* **2019**, *82*, 296–308. [\[CrossRef\]](#)
5. Zhang, P.; Huang, Y.F.; Wu, Y. Springback coefficient research of API X60 pipe with dent defect. *Energies* **2018**, *11*, 3213. [\[CrossRef\]](#)
6. Paiva, L.F.; Vaz, M.A. An empirical model for flexible pipe armor wire lateral buckling failure load. *Appl. Ocean Res.* **2017**, *66*, 46–54. [\[CrossRef\]](#)

7. Anderson, T.A.; Vermieya, M.E.; Dodds, V.J.N.; Finch, D.; Latto, J.R. Qualification of flexible fiber-reinforced pipe for 10,000-foot water depths. In Proceedings of the Offshore Technology Conference, Houston, TX, USA, 6–9 May 2013.
8. Pham, D.C.; Sridhar, N.; Qian, X.; Sobey, A.J.; Achintha, M. A review on design, manufacture and mechanics of composite risers. *Ocean Eng.* **2016**, *112*, 82–96. [[CrossRef](#)]
9. Dahl, C.S.; Andersen, B.; Groenne, M. Developments in managing flexible risers and pipelines, a suppliers perspective. In Proceedings of the Offshore Technology Conference, Houston, TA, USA, 2–5 May 2011.
10. Ebrahimi, A.; Kenny, S.; Hussein, A. Radial buckling of tensile armor wires in subsea flexible pipe—Numerical assessment of key factors. *ASME J. Offshore Mech. Arct. Eng.* **2016**, *138*, 031701. [[CrossRef](#)]
11. Drumond, G.P.; Geovana, P.; Pasqualino, I.P.; Pinheiro, B.C.; Estefen, S.F. Pipelines, risers and umbilicals failures: A literature review. *Ocean Eng.* **2017**, *148*, 412–425. [[CrossRef](#)]
12. API 17B. *Recommended Practice for Flexible Pipe*, 5th ed.; American Petroleum Institute: Washington, DC, USA, 2014.
13. Campello, G.C.; Sousa, J.R.M.; Vardaro, E. An analytical approach to predict the fatigue life of flexible pipes inside end fittings. In Proceedings of the Offshore Technology Conference, Houston, TX, USA, 2–5 May 2016.
14. Fernando, U.S.; Nott, P.; Graham, G.; Roberts, A.E.; Sheldrake, T. Experimental evaluation of the metal-to-metal seal design for high-pressure flexible pipes. In Proceedings of the Offshore Technology Conference, Houston, TX, USA, 30 April–3 May 2012.
15. Hatton, S.; Rumsey, L.; Biragoni, P.; Roberts, D. Development and qualification of end fittings for composite riser pipe. In Proceedings of the Offshore Technology Conference, Houston, TX, USA, 6–9 May 2013.
16. Peng, G.; Zhang, Z.; Li, W. Computer vision algorithm for measurement and inspection of O-rings. *Measurement* **2016**, *94*, 828–836. [[CrossRef](#)]
17. Liu, X.; Li, G.; Yue, Q.; Oberlies, R. Acceleration-oriented design optimization of ice-resistant jacket platforms in the Bohai Gulf. *Ocean Eng.* **2009**, *36*, 1295–1302. [[CrossRef](#)]
18. Tang, M.; Lu, Q.; Yan, J.; Yue, Q. Buckling collapse study for the carcass layer of flexible pipes using a strain energy equivalence method. *Ocean Eng.* **2016**, *111*, 209–217. [[CrossRef](#)]
19. Cour, D.; Kristensen, C.; Nielsen, N.J.R. Managing fatigue in deepwater flexible risers. In Proceedings of the Offshore Technology Conference, Houston, TX, USA, 5–8 May 2008.
20. Li, X.; Jiang, X.; Hopman, H. A review on predicting critical collapse pressure of flexible risers for ultra-deep oil and gas production. *Appl. Ocean Res.* **2018**, *80*, 1–10. [[CrossRef](#)]
21. Wang, L.Q.; Wei, Z.L.; Yao, S.M.; Guan, Y.; Li, S.K. Sealing performance and optimization of a subsea pipeline mechanical connector. *Chin. J. Mech. Eng.* **2018**, *31*, 1–14. [[CrossRef](#)]
22. Fernando, U.S.; Karabelas, G. Analysis of end fitting barrier seal performance in high pressure un-bonded flexible pipes. In Proceedings of the 33rd ASME International Conference on Ocean, Offshore and Arctic Engineering, San Francisco, CA, USA, 8–13 June 2014.
23. Li, X.; Du, X.; Wan, J.; Xiao, H. Structure analysis of flexible pipe end fitting seal system. In Proceedings of the 34th ASME International Conference on Ocean, Offshore and Arctic Engineering, St John's, NL, Canada, 31 May–5 June 2015.
24. Zhang, L.; Yang, Z.; Lu, Q.; Yan, J.; Chen, J.; Yue, Q. Numerical simulation on the sealing performance of serrated teeth inside the wedgy sealing ring of end fitting of marine flexible pipeline. *Oil Gas Storage Transp.* **2017**, *37*, 108–115. (In Chinese)
25. Marion, A.; Rigaud, J.; Werth, M.; Martin, J.  $\gamma$ -Flex®: A new material for high temperature flexible pipes. In Proceedings of the Offshore Technology Conference, Houston, TX, USA, 6–9 May 2002.
26. API 17J. *Specification for Un-Bonded Flexible Pipe*, 4th ed.; American Petroleum Institute: Washington, DC, USA, 2014.
27. Yan, H.; Zhao, Y.; Liu, J.; Jiang, H. Analyses toward factors influencing sealing clearance of a metal rubber seal and derivation of a calculation formula. *Chin. J. Aeronaut.* **2016**, *29*, 292–296. [[CrossRef](#)]
28. Gorash, Y.; Dempster, W.; Nicholls, W.D.; Hamilton, R. Fluid pressure penetration for advanced FEA of metal-to-metal seals. *Proc. Appl. Math. Mech.* **2015**, *15*, 197–198. [[CrossRef](#)]
29. Zhao, B.; Zhao, Y.; Wu, X.; Xiong, H. Sealing performance analysis of P-shape seal with fluid pressure penetration loading method. *IOP Conf. Ser. Mater. Sci. Eng.* **2018**, *397*, 012126. [[CrossRef](#)]



30. Slee, A.J.; Stobart, J.; Gethin, D.T.; Hardy, S.J. Case study on a complex seal design for a high pressure vessel application. In Proceedings of the ASME Pressure Vessels and Piping Conference, Anaheim, CA, USA, 20–24 July 2014.
31. Wang, B.; Peng, X.; Meng, X. A thermo-elastohydrodynamic lubrication model for hydraulic rod O-ring seals under mixed lubrication conditions. *Tribol. Int.* **2019**, *129*, 442–458. [[CrossRef](#)]
32. Deng, D.; Zhang, C.; Pu, X.; Liang, W. Influence of material model on prediction accuracy of welding residual stress in an austenitic stainless steel multi-pass butt welded joint. *J. Mater. Eng. Perform.* **2017**, *26*, 1494–1505. [[CrossRef](#)]
33. Yu, C.; Heinrich, J. Petrov-Galerkin methods for the time-dependent convective transport equation. *Int. J. Numer. Meth. Eng.* **1986**, *23*, 883–902. [[CrossRef](#)]
34. Yu, C.; Heinrich, J. Petrov-Galerkin method for multidimensional, time-dependent, Convective-Diffusive equations. *Int. J. Numer. Meth. Eng.* **1987**, *24*, 2201–2215. [[CrossRef](#)]
35. Yu, R.; Yuan, P. Structure and research focus of marine un-bonded flexible pipes. *Oil Gas Storage Transp.* **2016**, *35*, 1255–1260. (In Chinese)
36. Malta, E.; Martins, C. Finite element analysis of flexible pipes under axial compression: Influence of the sample length. *ASME J. Offshore Mech. Arct. Eng.* **2017**, *139*, 011701. [[CrossRef](#)]
37. Cuamatzi-Melendez, R.; Castillo-Hernandez, O.; Vazquez-Hernandez, A.O.; Vaz, M.A. Finite element and theoretical analyses of bisymmetric collapses in flexible risers for deepwaters developments. *Ocean Eng.* **2017**, *140*, 195–208. [[CrossRef](#)]
38. Pethrick, R.A.; Banks, W.M.; Brodesser, M. Ageing of thermoplastic umbilical hose materials used in a marine environment 1-Polyethylene. *Proc. Inst. Mech. Eng. Part L J. Mater. Des. Appl.* **2014**, *228*, 45–62. [[CrossRef](#)]



© 2019 by the authors. Licensee MDPI, Basel, Switzerland. This article is an open access article distributed under the terms and conditions of the Creative Commons Attribution (CC BY) license (<http://creativecommons.org/licenses/by/4.0/>).